Scalable graphene production: perspectives and challenges of plasma applications

DOI: 10.1039/c5nr06537b

Igor Levchenko, Kostya (Ken) Ostrikov, Jie Zheng, Xingguo Li, Michael Keidar, and Ken Teo

Graphene, a newly discovered and extensively investigated material, has many unique and extraordinary properties which promise major technological advances in the fields ranging from electronics to mechanical engineering and food production. Unfortunately, complex techniques and high production cost hinder commonplace applications. Scaling of existing graphene production techniques to the industrial level without compromising its properties is a current challenge. This article focuses on the perspectives and challenges of scalability, equipment, and technological perspectives of the plasma-based techniques which offer many unique possibilities for the synthesis of graphene and graphene-containing products. The plasma-based processes are amenable for the scaling and could be also useful to enhance the controllability of the conventional chemical vapour deposition and some other techniques, and to ensure a good quality of the produced graphene. We examine the unique features of the plasma-enhanced graphene production approaches, including the techniques based on inductively-coupled and arc discharges, in the context of their potential scaling to mass production following the generic scaling approaches applicable to the existing processes and systems. This work analyses a large amount of recent literature on graphene production by various techniques and summarizes the results in tabular form to provide a simple and convenient comparison of several available techniques. Our analysis reveals a significant potential of scalability for plasma-based technologies, based on the scaling-related process characteristics. Among other processes, greater yield of 1 $g \times h^{-1} m^{-2}$ was reached for arc discharge technology, whereas the other plasma-based techniques show process yields comparable with the neutral-gas based methods. Selected plasma-based techniques show lower energy consumption than in thermal CVD processes, and the ability to produce graphene flakes of various sizes reaching hundreds of square millimetres, and thickness varying from monolayer to 10-20 layers. Additional factors such as electrical voltage and current, not available in thermal CVD processes could potentially lead to better scalability, flexibility and control of the plasma-based processes. Advantages and disadvantages of various systems are also considered.

1 Introduction

According to data provided by the *UK Intellectual Property Office Informatics Team*, the number of patent publications on graphene[1] for 2005-2014 exceeded 25,000,[2] with 2014 being a peak publication year. It is naturally expected that the publication rise will continue in 2015 and beyond. In comparison, only about 50 patent applications were lodged 10 years ago. The graph illustrating the time dependence of the patent applications and granted patents for several important materials, including silicon, carbon nanotubes and graphenes, is shown in Fig. 1.[3] This patenting "wave" is due to a whole spectrum of the unique properties pertinent to graphene and related structures such as carbon nanotubes,[4] fullerenes,[5] nanoribbons,[6] and some other nano-carbon materials. Indeed, the graphene and related materials are attractive candidates for a wide range of applications, starting from the graphene-based electronic devices utilizing the presence of topologically protected edge states in zig-zag graphene,[7] and ending with the structural materials,[8] biomedical devices,[9] and biosensors.[10] Graphenes for the flexible displays,[11] dye-sensitized solar cells,[12] electrifying inks,[13] electrochemical energy storage devices,[14,15] corrosion protection,[16] aerospace applications,[17] light-emitting diodes,[18] advanced field-effect transistors[19] and various bioinspired structural materials[20] also represent important niches for the application of two-dimensional carbon materials.

Yet the high promises of graphene have not yet been fully materialised despite many impressive achievements. Up to date, the problem of the production of large quantities of high-quality graphenes is one of the main challenge limiting its industrial applications. One of the key reasons is that it is very difficult to retain the structural integrity and quality of the most common types of graphenes (such as graphene films or flakes, substrate-supported or free-standing) upon *scaling-up* of the laboratory tested methods and techniques. Another issue is a relatively high cost of the graphene production. Considerable progress in the cost reduction in graphene fabrication at the laboratory scale was obtained in several past years.[3] However, further advances are needed to make graphene-based processes and products technologically and commercially viable. The cost of precursor materials is a substantial part of the total graphene costs; as a result, a wide search for the cheap, commonly available, natural

precursors is in progress.[21,22] Nevertheless, the available state-of-the-art is not fully ready for industrial applications, and new innovative approaches are actively sought.

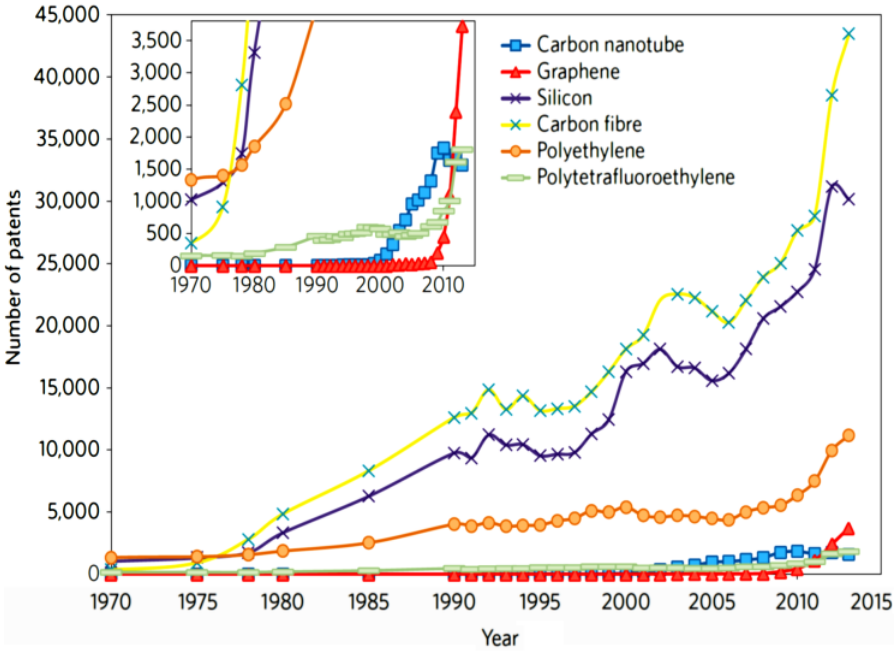

Fig. 1 Number of patent applications and granted patents by first publication date. Reprinted with permission from A. Zurutuza et al., Nature Nanotech. 9, 2014, 730. Copyright 2014, Nature Publishing Group.

Here we present a short review focused specifically on the perspectives and challenges of scalability, equipment, and technological perspectives of the graphene production, with the main attention paid to the plasma-based techniques. This work does not aim to exhaustively examine the physical, chemical, mechanical and many other processes involved in graphene nucleation, growth, collection, purification etc.; instead, we critically analyse three typical kinds of graphene (specifically, unsupported graphene flakes, vertically-oriented surface-supported graphene walls, and graphene films on solid surfaces), as well as various growth techniques with the aim to find out how plasmas can be used to enhance the existing methods or form the basis of alternative approaches to scaling graphene production. The issues of the process controllability by varying the plasma discharge parameters are also considered. We also

stress that the numerous processes involved in the graphene formation[23] including the plasma-related processes[24,25] are discussed in great details in many reviews and original papers.[26,27]

We should mention that nucleation and growth of graphene requires specific conditions, namely relatively high energy of particles involved in the graphene formation, as well as precisely tuned flux of material in the reactor chamber. These conditions can be satisfied in the plasma-based methods by the proper selection of the plasma parameters (electron, atom, and ion temperature, plasma density, surface potential, current through plasma and others).[28,29] Along with this, the plasma is a very complex environment which involves many processes not found in the neutral-gas based reactors, such as electric-field induced diffusion, plasma-surface interaction, self-organization on plasma-exposed surfaces and many others. As it was mentioned above, our review is primarily focused on the scalability and industry-oriented approaches and concepts, and thus many plasma-intrinsic processes and effects are outside the scope of this paper. The interested reader can refer to numerous specialized review and research papers addressing the specific processes in plasma.[30,31,32]

One more aspect to be addressed is the difference between the thermal and non-thermal plasmas involved in graphene production. Indeed, thermal plasmas produced by cathodic and anodic arcs, and non-equilibrium low-temperature plasmas produced by, e.g. radio-frequency or magnetron discharges are quite different environments that involve different physical and chemical processes. Specifically, thermal plasmas demonstrate very high (possibly near 100 %) ionization degree and low electron temperature,[33] whereas non-equilibrium non-thermal plasmas is a weakly (up to several %) ionized environment with relatively high (up to several tens of electron-volts is some cases) electron energy.[34,35,36] This difference will have a major effect on the graphene nucleation and growth, equipment architecture and graphene properties. Indeed, much higher pressures, as well as heat fluxes and material supply rates lead to much faster (fraction of seconds) formation of graphene flakes, whereas the growth in low-temperature non-equilibrium plasmas may take minutes and even hours. In our review we will briefly mention these differences, but again the reader should refer to special reviews and research papers to address these specific questions (including effect of the specific plasma parameters on the graphene characteristics) which are apparently out of the scope of our paper.[37,38]

Table 1 summarizes the interrelation between the specific plasma processes and important graphene characteristics.

Table 1. Typical graphene flake sizes for various production techniques

Method	Type	Size	Number of layers	Ref.
Thermal plasma jet	Unsupported graphene flakes (quantum dots)	10-20 nm	Monolayer	[39]
Growth on SiC (thermal annealing)	Graphene film	300 µm	Monolayer	[40]
Laser irradiation	Graphene oxide grains on surface	0.5-5 µm	Monolayer	[64]
Exfoliation	Unsupported flakes	1-2 µm	1 – 2	[41]
Chemical cutting	Graphene quantum dots	8 µm	Up to 7	[42]
CVD	Graphene crystals on Cu	0.5 mm	Monolayer	[43]
CVD	Graphene crystals on Ni	1 cm^2	1 to 12	[44]
2-step CVD	Film on Cu	142 μm^2	1 – 2	[45]
Low-pressure CVD (LPCVD)	Graphene crystals on Cu	0.5 mm	Monolayer	[46]
PECVD (inductively oupled plasmas, ICP)	Graphene flakes on Si nanograss	10 µm	2 to 6	[47]
PECVD	Grains on Cu	1-3 µm	Monolayer	[48]
PECVD	Vertical sheets	3-5 µm	3 – 4	[49]
PECVD (microwave)	Graphene film on Cu	100 mm^2	Monolayer	[50]
PECVD (ICP), no metal catalyst	Graphene flakes on Si nanograss	5 µm	2 to 9	[51]
PECVD (ICP)	Vertically-aligned flakes on nanopores	1 µm	10 to 20	[52]
PECVD, natural precursors	Vertically-aligned graphene flakes	10 µm	3 - 10	[21]
DC arc discharge in CO_2	Graphene sheets	500 nm	4 – 5	[53]
Arc discharge	Unsupported flakes	200 nm	2 – 4	[54]
Helium arc discharge	Unsupported graphene sheets	1 µm	1 – 10	[55]
Pulsed arc in H_2O	Unsupported nanoflakes	1-2 µm	2 – 5	[56]

Arc + ZnS as catalyst	Unsupported nanoflakes	Tens of μm	2 – 7	[57]
Magnetically enhanced arc	Unsupported flakes	0.5 – 2.5 μm	1 – 10	[58]

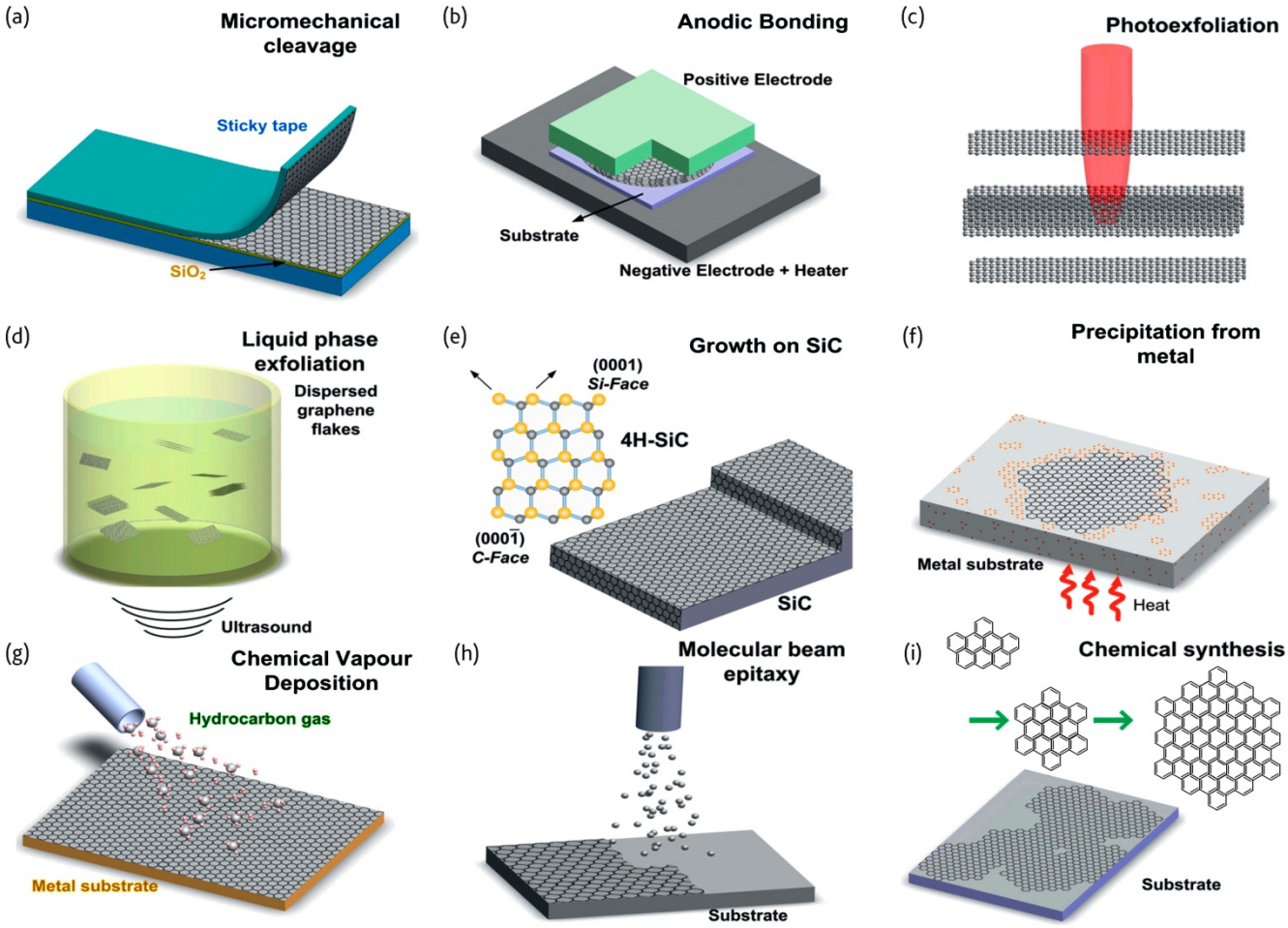

Fig. 2 Schematics of representative graphene fabrication techniques. Reprinted with permission from F. Bonaccorso et al., Mat. Today 15, 2012, 564–589. Copyright 2012, Elsevier Ltd.

Mechanical exfoliation (micromechanical cleavage)[59] and chemical vapour deposition[60,61] (CVD) are among the earliest techniques to produce small pieces (flakes) of single- and few-layer graphenes. Other methods such as anodic bonding,[62,63] photoexfoliation,[64] metal precipitation,[65,66,67] and liquid phase exfoliation[68,69] were developed and demonstrate reasonable purity of the product, high crystallinity and low defect levels. Figure 2 summarizes the selected common approaches to the graphene fabrication,[70]

and Table 1 lists the most popular graphene production methods and the characteristic sizes of graphene flakes typical for each method.

Among other methods, CVD-based techniques have attracted a strong interest for the possible scalable graphene production. Earlier efforts to scale up CVD graphene production have been very promising, yet required much higher production rates.[71,72] Other approaches such as exfoliation in liquids[73,74] and template method,[75] also could be considered as promising for scaling, but require further improvement. There is a scope for increasing the throughput and production rate/scale of graphene without compromising the graphene quality and structure.

Low-temperature plasma-enhanced CVD (PECVD) may be suitable for high-yield graphene production. Indeed, PECVD is now a subject of a strong interest from academic and industry sectors because of its capacity to produce large quantities of carbon nanostructures of high quality in a controlled environment[76,77] owing to quite different, as compared with the traditional CVD, process parameters. The PECVD technique is promising for large production yields due to high rates of material supply and hence, high rates of graphene synthesis. Plasmas can significantly complement and advance CVD-based processes, thereby helping to reach the production rates and costs appropriate for commercial graphene applications. Indeed, graphene synthesis requires special environment with appropriately high but not excessive energy of particles involved in the graphene growth, sophisticatedly balanced supply of carbon to the growing graphene, and in some cases, a purposely activated catalyst.[78,79] In the CVD process, relatively high temperature reaching 1000-1200 °C is used. When plasma is a process environment, these conditions are ensured by an appropriate selection of the process parameters such as plasma density, temperature of electrons in plasma, and electric potential on the growth surface. The arc and inductively-coupled discharges are capable of generating high-density plasmas, and hence these two techniques are particularly promising for the scalable graphene fabrication.

A sequence of complex processes including dissociation of the carbon-containing precursors (acetylene, methane, ethanol, carbon dioxide ethylene), supply of the carbon-containing precursor to the growth surface, and various processes on the surfaces leading to the grain nucleation and growth.[80,81,82]

is involved in CVD technique. The growth of graphenes occurs due the atom supply directly from the gas phase or by the surface diffusion[83,84] and further their incorporation into the growing graphene structure.[85,86] Control over these processes is a challenge, and plasma-based CVD processes are considered to enhance the controllability with respect to the position, size and shape of the growing films/flakes, to increase the growth rate and to lower the surface temperature. The plasma can be considered as a process environment capable to control the processes involved in the graphene formation.

The presence of electrons and ions in plasma provides a possibility to control the process, including material fluxes, by electric and magnetic fields. Numerous experimental and theoretical studies have confirmed a quite high level of control over the structure and growth rates of the nanomaterials grown in plasma environments.[87,88] Other important feature of the plasma-based processes include the lower temperatures required for the graphene nucleation and growth.

This is why plasma-based methods have attracted interest for the scalable graphene synthesis.[89] Various kinds of graphene and related materials were fabricated in the setups potentially amenable for scale-up, including vertically oriented graphene nanosheets,[90,91] single-layer graphenes on a Cu foil,[48] and unsupported graphene and carbon nanotubes in arc discharge plasmas.[92] The latter process features a single-step synthesis and magnetic purification and is thus of a special interest for the scaled graphene production. It should be noted that further graphene modification and functionalization, e.g., nitrogen doping, intentional defect creation, etc. could also be effectively implemented during the plasma-based fabrication.[93]

Energy required for the graphene synthesis is another important aspect directly influencing the selection of the most appropriate production technique. CVD-based processes quite often include long periods of heating up, slow growth and long cooling. This usually leads to a substantial waste of energy. With the plasma-based technique, the process can be instantaneously switched on or off, where energy is provided by the plasma. Thus, the long heating of the furnace in not required, and the material deposition and graphene growth can be activated immediately upon ignition of the discharge where the particles are formed and then deposited onto the electrically biased substrate (both external and self-bias

are possible). One typical example of the energy-wise plasma-based process is the nanosecond spark technique where the energy is purposefully supplied in nanosecond intervals.

Table 2. Energy cost of incorporating each atom into the nanostructure in various techniques.

Source	Average power, W	Energy cost, eV	Ref.
Thermal furnace	5000	1.2×10^{8}	94, 101
Microplasma	20 – 50	$10^{3} – 6\times10^{5}$	95, 96, 97, 98
DC arc	120	5×10^{4}	99
Microsecond spark	1.5	1500	100
Nanosecond spark	1 – 4	75	94

Let us examine the energy required for an atom to incorporate into the growing nanostructure in different processes, including CVD. One should consider the energy required to yield carbon-containing atoms, transport them to the growth area, and incorporate them into the growing structure. Table 2 shows this minimum energy calculated for several nanoscale synthesis processes including thermal CVD process conducted in a single-zone heating furnace, as well as several plasma-based methods such as microplasma, DC arc, microsecond spark and nanosecond spark techniques. The method of calculation of the numbers listed in Table can be found elsewhere.[101] Note that the energy costs for all techniques listed in Table 2 were calculated with the assumption that all material produced in the discharge was transformed into the graphene flakes. From this table one can see that some kinds of plasmas indeed demonstrate low energy consumption for the atom to incorporate in the nanostructure. We stress that the values listed in Table 2 where calculated using the results obtained in small-scale (laboratory) experiments, and more work is required to demonstrate this possibility at larger production

scales.

Table 3. Typical graphene production yields for various fabrication techniques (calculated from references listed in Table).

Method	**Type**	**Yield**	**Ref.**
CVD	Graphene flakes (nanowalls) on surface	0.005-0.01 $g \times h^{-1} m^{-2}$	[102]
Arc discharge	Unsupported flakes	1 $g \times h^{-1} m^{-2}$	[58]
ICP technology	Graphene flakes (nanowalls) on surface	0.01 $g \times h^{-1} m^{-2}$	[47]
CVD	Surface-supported graphene film	10^{-5}-10^{-4} $g \times h^{-1} m^{-2}$	(*)

(*) Calculated as a mass of monolayer graphene film grown in a typical CVD process during 2-3 h.

Let us consider various processes in terms of their potential for mass production by comparing the production yields achieved in the neutral-gas and plasma-based techniques. The typical values calculated from the published information are listed in Table 3. The data listed in the table show that the yields obtained in laboratory experiments demonstrate considerable potential of the plasma-based methods. Again, more experiments are required to confirm this tendency during scaling up.

2 Three graphene types – films, supported oriented flakes, unsupported flakes

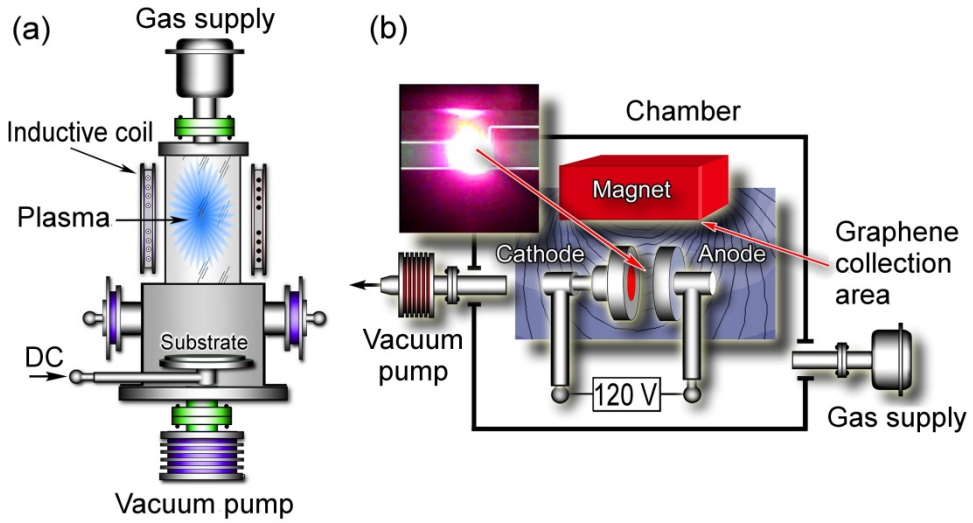

Fig. 3 (a) Schematic of the ICP reactor with the coil installed over the plasma confinement chamber. Reprinted with permission from Levchenko et al., J. Vac. Sci. Technol. B 2013, 31, 050801. Copyright 2013, AIP. (b) Schematic of the arc discharge experimental setup and photo of the discharge (inset). Graphene flake-containing material was collected from the magnet surface (collection area), located close to the discharge. A simulated two-dimensional map of the magnetic field is shown on the background of the discharge. Reprinted with permission from Levchenko et al., Carbon 48, 4556 (2010). Copyright 2010, Elsevier Ltd.

Graphenes are commonly produced (by any methods including the plasma-based techniques) in the three common forms: films laying supported by smooth substrates (e.g., silicon carbide[89] or metal[103]) (i), oriented (e.g., vertically-aligned) flakes, or nanowalls[90] supported by diverse substrates (ii), and unsupported flakes (iii) that deposit on the chamber walls or collection surfaces,[92] and can be used to produce liquid suspensions[104]. Plasma-based methods are able to produce all these three types of graphenes. For example, the inductively-coupled plasma (ICP) reactor (Fig. 3a) is one of the most

promising setups for the fabrication of vertically-aligned graphene flakes, although similar structures have been achieved using other types of plasma discharges (e.g, DC[105] or microwave[106,107]). Another example is the unsupported graphene flakes which are commonly produced by the setups based on arc discharges in the relatively high (up to atmospheric) pressure gas environments (Fig. 3b), whereas the conventional plasmas (for example, microwave[108]) is also capable of producing such structures. Importantly, the arc discharge in vacuum or controllable gas atmosphere under reduced pressure conditions is one of the most promising techniques for the large-scale production of various nano-materials with minimal structural defects. This method combines a large yield with a relatively high controllability.[109,110]

Below we will examine in detail only two commonly used plasma-based techniques capable of producing graphene flakes, namely those based on arc discharge (AD) and inductively coupled plasmas (ICPs). The AD and ICP technologies appear to be suitable for automation and scaling into the industrial yields, mainly due to their simplicity, controllability and high intrinsic yield. Importantly, each of these two techniques (AD and ICP) is capable of producing all the three above introduced types of graphenes – continuous films supported by smooth substrates, oriented (including vertically oriented) flakes supported by diverse substrates, and unsupported flakes.

2.1. Graphene production using arc discharge plasma

Figure 3b shows a setup for the arc discharge-assisted fabrication of unsupported graphene flakes. The anode temperature reaches 3500 K[111] in this discharge, and dense thermally-equilibrium plasma is produced by intense erosion of electrode material in the discharge spots.[112] The gas temperature in the discharge core reaches 5000 K. Therefore, the graphene flakes can be effectively heated up to the temperatures required for the efficient graphene formation even if they pass the reaction zone at a very high speed (typically, for 10^{-4} s [113]). An external magnetic field created with the help of external magnetic coil or magnet above the process area significantly enhances the plasma density due to the magnetic confinement that holds the plasma near electrodes, and due to the magnetization of plasma electrons which promotes ionization of the neutral atoms.[114] The electron temperature also increases due

to stronger electric field in the magnetized plasma, thus resulting in stronger graphene heating in the plasma and intense material flux to the graphene surfaces. Consequently, efficient nucleation, fast growth and high crystallinity of the graphene flakes are ensured. It should be noted that an external magnetic field is not absolutely necessary for the graphene fabrication in arc plasma, and efficient synthesis can be ensured by proper arrangement of the plasma fluxes.[115]

Graphene is produced in the arc discharge-based process with carbon anode/cathode assembly mounted in a vacuum chamber.[116] The anode is in the form of a hollow rod filled with a mixture of graphitic carbon and catalyst (for example, Y and Ni powders). The cathode is a solid graphite cylinder. The cathode to anode gap is varied in the range of 1–5 mm, depending on the discharge current. Typically, the chamber is filled with helium at a pressure of 200–500 Torr.[117] A representative topography of the magnetic field produced by the cube-shaped permanent magnet installed in the chamber is shown in Fig. 3b. The gas temperature in the magnetically enhanced plasma reaches 5000 K, and the metal catalyst particles emitted to the plasma from the electrode evaporate.[118] Later, the metal catalyst re-nucleates into nanoparticles of several nm in diameter, and the graphene flakes nucleate and grow on them when the temperature falls below 1500 K. More details on the setup design and process parameters can be found elsewhere.[58] Catalyst powder also may be avoided by using, e.g., heated copper collection surfaces.[119]

Figure 4a is the schematic illustrating the process for the growth of graphene flakes in arc discharge followed by the preparation of a liquid suspension. The process starts from loading the catalyst powder into anode and anode installation into the chamber. At the end of the process, carbon deposit is collected from the chamber and sonicated to separate the graphene flakes from the rest carbon deposited on the collection surfaces (note that this process allows for the separation of graphene and carbon nanotubes which are also useful by-products of the reaction). The sonification produces a graphene suspension, which could be used, e.g., for the production of the printable graphene-containing inks.[120]

The arc-produced graphene flakes were characterized using the SEM, TEM, AFM, and micro-Raman techniques, and the results of the characterization are shown in Fig. 5. The size of the arc-produced graphene flakes reached 2.5 μm, with the number of layers ranging from 3 to 10, whereas the samples

collected directly from the magnet surface contained up to only 3 layers. This result was also confirmed by the AFM technique which has demonstrated the height of the graphene flakes of 1.5 nm. The defect level of the graphene flakes collected from the magnet and chamber walls was characterized using the micro-Raman technique. The specimens collected from the magnet surfaces have demonstrated a weak D-peak at around 1325 cm^{-1}, indicating a low amount of defects in sp^2 bonds. The 2D-peak present in Figure 5 is caused by scattering of phonons with the opposite wave vectors, so it is not a signature of the defect level in the sample. Moreover, the SAED pattern produced in a TEM microscope using the sample collected on the magnet surface revealed the pattern expected for a hexagonal close-packed crystal.

2.2. Graphene fabrication using ICP plasma

PECVD process can produce structure-controllable networks of high-quality graphene,[88,121] owing to the increased temperature, as well as intense ion and electron irradiation which activate the graphene edges and promote incorporation of carbon atoms and ions into the structure of the growing graphene flakes.[122,123] The graphenes fabricated using, for instance, the inductively-coupled plasma method exhibit two different morphologies, namely (i) small flakes[124] grown on silicon wafer without the use of any metal catalysts (this feature is important for some biotechnological applications), and (ii) turnstile-like and maze-like structures. Thus, the process parameters are very important for the deterministic growth of the two types of structures.[125,126]

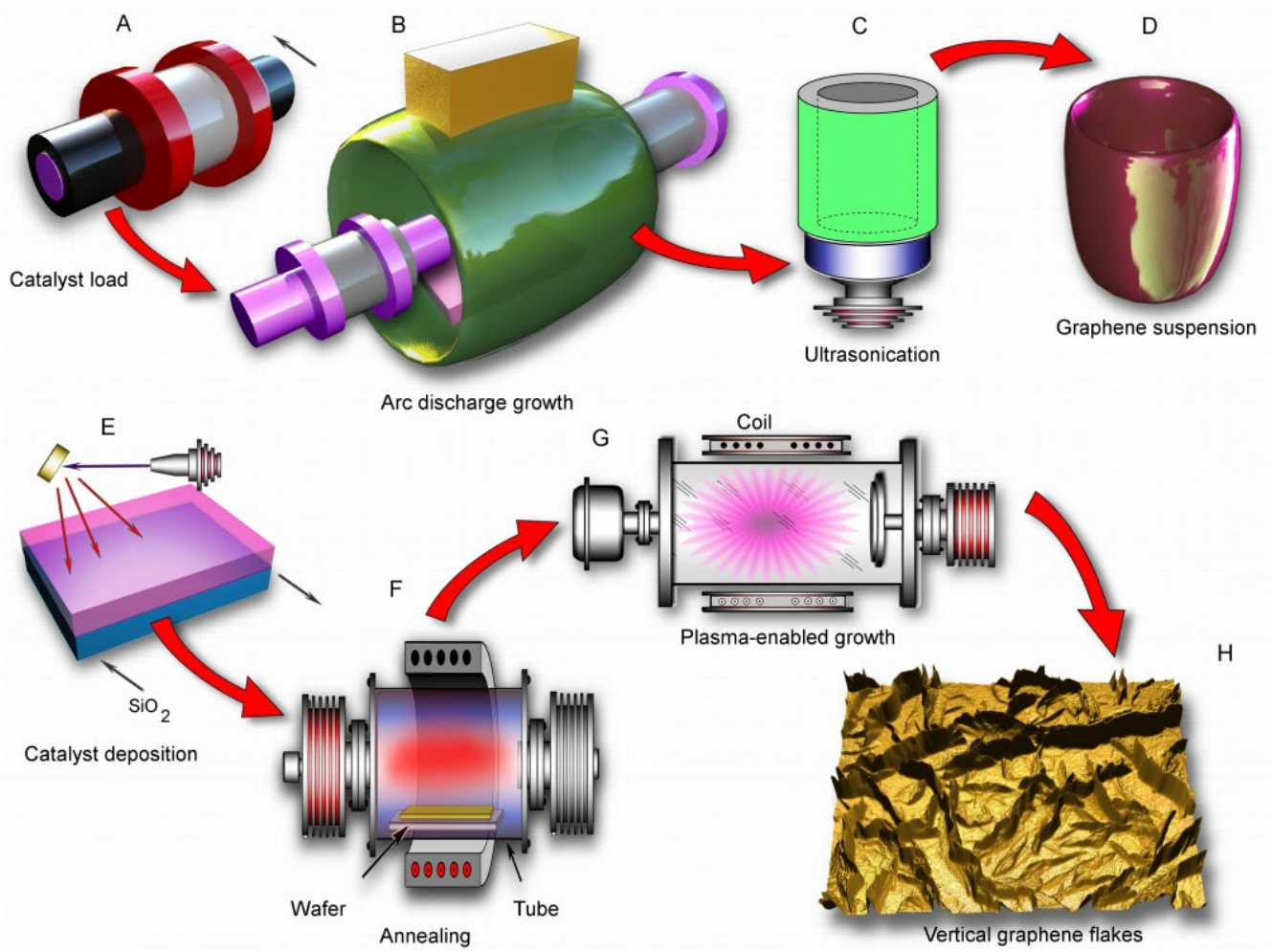

Fig. 4 (A-D) Schematics of graphene flake fabrication in arc discharge and (E-H) ICP plasma. Both processes include several stages, the most important being process preparation (e.g., catalyst preparation and loading) (A, E), graphene synthesis (B, F, G), product collection, separation (C, H) and purification (D).

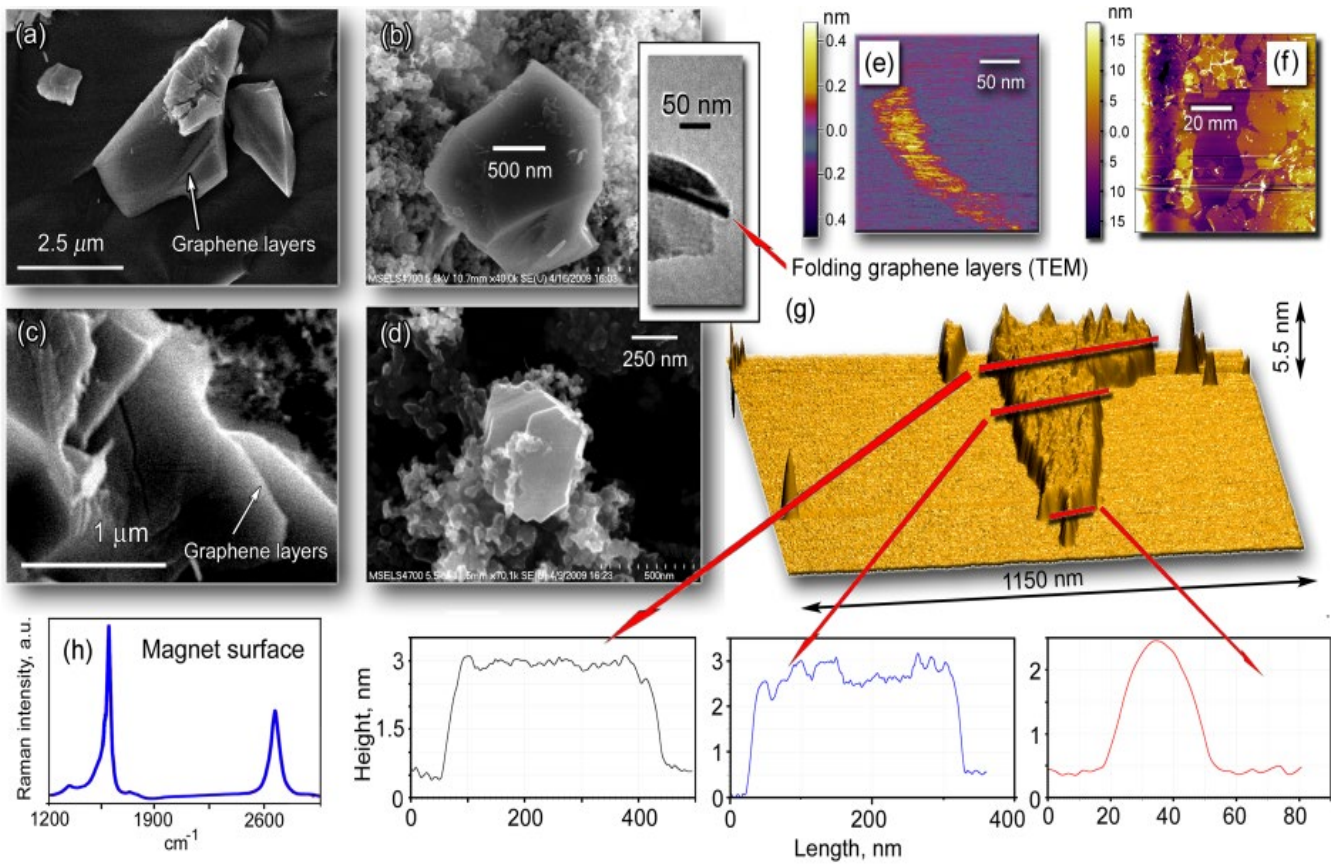

Fig. 5 Scanning electron microscopy (SEM), transmission electron microscopy (TEM), atomic force microscopy (AFM), and Raman characterization of the pristine [(a) and (b)] and processed [(c) – (g)] samples collected from the surfaces of a magnet installed in a vacuum arc discharge. Representative SEM images of the carbon nanoparticles containing graphene flakes [(a) and (b)]; SAED pattern of the carbon material (c); TEM image of the folding graphene layers (d); 2D [(e) and (f)] and 3D (g) AFM images of two graphene flake samples. Three profiles of the AFM image illustrate the flake structure containing several graphene layers (total thickness 2–3 nm); Representative Raman spectra of the graphene flake samples (h). G-peak at ≈1582 cm^{-1} and symmetrical 2D-peak at 2650 cm^{-1} demonstrate the presence of a relatively small number of graphene layers in the flakes. Reprinted with permission from Levchenko et al., Carbon 48, 4556 (2010). Copyright 2010, Elsevier Ltd.

Different types of plasma systems such as magnetron-based[127,128,129] or inductively and capacitively coupled plasma-enhanced chemical vapour deposition have the features capable of satisfying the process requirements[130,131] In one of the typical processes (ICP-CVD, with the frequency of 13.56 MHz and discharge power of about 1.0 kW, mixture of CH_4 and H_2 in Ar was used), the growth was carried out in a plasma generated in the pressure range of 1-5 Pa, discharge power of about 700 W and using DC bias of -60 V applied to the substrate. No external heating was used, and the plasma heating by the ion and electron irradiation generated the required graphene growth temperature (approx 700 K) on the silicon wafer thermally oxidized prior to the growth of oriented graphenes. This typical process usually results in the formation of high-quality maze-like vertically-oriented graphene structures, sometimes called graphene or carbon nanowalls.[27]

Growth of such graphene structures in the plasma environment on nanoporous substrates instead of solid silicon wafers also offers enhanced controllability of the process and a relatively high production yield. Figure 6 shows the results of low- and high-resolution SEM characterization and Raman spectra of the vertically-aligned graphene flakes grown on nanoporous aluminium oxide (Al_2O_3) substrates in the low-temperature plasma environment under different conditions. According to the results of the Raman measurements, the defect level of these samples is less than 10^{13} cm^{-2} (1%), i.e. it is quite low. Indeed, it was demonstrated that the graphene mechanical properties are compromised when the defect level is within 5%.[132] On the other hand, this defect level is high enough to ensure a significant magnetic moment, and thus, the reported graphene flakes are quite attractive for the potential magnetic applications. TEM analysis using a 200 keV electron beam has shown that the flakes consist of 10-20 single graphene layers. The comparison of the peak intensity ratios of D and G bands was also made to quantitatively characterize the quality of the fabricated graphenes. It is known that the larger D/G ratio indicates the presence of defects. Plasma-fabricated graphene flakes gave demonstrated reasonably low D/G ratio numbers. A comparison of 2D and D band ratios which indicates the number of graphene layers was also made, and the plasma treated samples have demonstrated significantly thinner nanowalls with 2D/G = 0.75. More details can be found elsewhere.[52]

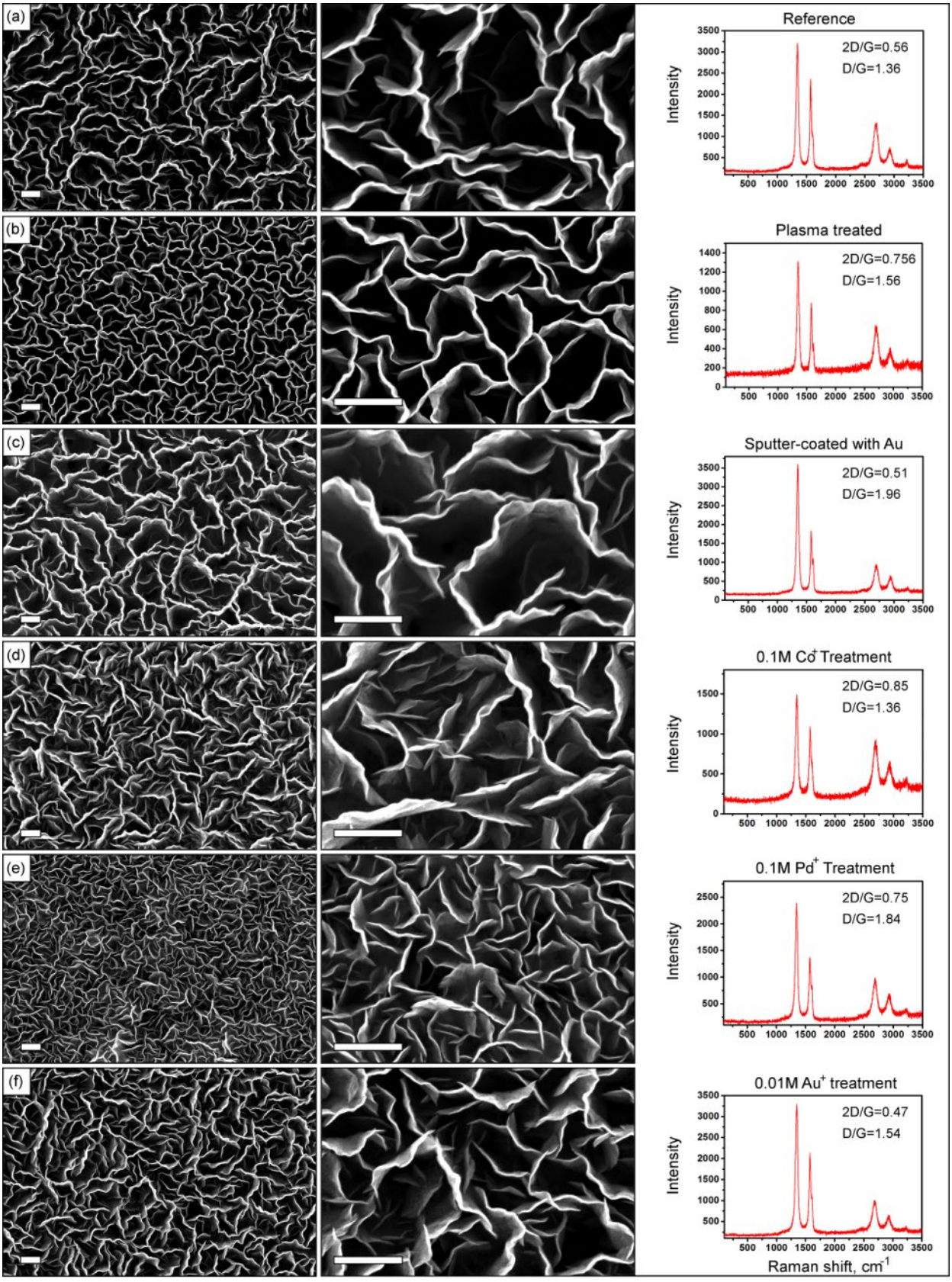

Fig. 6 Low- and high-resolution SEM images and Raman spectra of the vertically oriented graphene sheets grown on nanoporous alumina substrate in the low-temperature plasma environment under the following conditions: $CH_4/Ar/H_2$ ratio – 2:1:1, chamber pressure – 3.0 Pa, RF power – 850 W, treatment time – 6 min. Images (a-f) correspond to different treatment processes and catalysts used. Scale bars are 500 nm. Reprinted with permission from Fang et al., Sci. Technol. Adv. Mater. 15, 055009 (2014). Copyright IOP 2014.

3 Scale-up considerations

Let us now discuss generic approaches that may be suitable for the scaling up of the graphene production techniques. We do not aim here to present a comprehensive review of the recent efforts for scaling the graphene production. Instead, we will focus on two processes of interest, namely the arc discharge and ICP-based methods and examine specific options for scaling them up.

The presently developed CVD techniques, along with several other methods (including the methods summarised in Fig. 2) are more suitable for the discrete batch-type processes. In this type of processes, a substrate or precursor material is loaded into a batch chamber, then coated, and subsequently unloaded from the reactor, after the process is completed. This sequence is repeated thereby leading to a "discrete" process which involves significant interruptions between the process steps. Continuous processes represent another type of scalable processes and usually involve continuous loading and removal of materials. From this point of view, scaling up graphene production may be based on the following approaches:

1. In the case of discrete (batch) process, the scaling is achieved by enlarging the fabrication facility to a large size where a large number of the growth substrates (e.g., catalysts) is placed at the maximum possible loading without compromising the quality and yield of the resultant graphene-based structures. A representative example of this type of processes is the plasma-based growth of surface-supported films and structures made of various semiconducting and dielectric materials on large (up to several square meters[133]) panels;

2. If the case of the continuous process where precursor is fed and the graphene materials are produced, purified, and collected continuously, the scaling may be achieved by enlarging the fabrication facility (similar to case 1 above), as well as by improving the throughput of the process by achieving higher growth rates, higher speeds of material supply and product removal, etc. The production of unsupported graphene flakes by arc-discharge based technique, and roll-to-roll (R2R) techniques are typical examples of this approach. Below we will examine these examples in more details.

4 Examples of realization and possible design solutions

Let us first consider a typical, continuous roll-to-roll (R2R) manufacturing equipment utilizing conventional chemical vapour deposition.[134] Such a system usually consists of a vacuum chamber, a winder and re-winder, as well as a pair of current-feeding electrode rollers (Fig. 7a). In this system, a large area of a copper foil can be selectively heated between the current-feeding rollers to a temperature of ≈1000 °C. Typically, a cold-rolled copper foil of 200 mm width with the length exceeding 100 m was used. The pressure during the process is maintained at 1000 Pa under a continuous flow of methane and hydrogen. An elevated pressure in the process chamber suppresses copper sublimation. The foil was transported through the roll-to-roll system at a velocity of about 10 $cm \times min^{-1}$, so the process duration exceeded 16 h. After the growth, additional processes are required to separate the graphene from the Cu foil and put it onto its final substrate (polyethylene, PET) as shown in Figs. 7b, c, and d. Figure 7b illustrates the reverse gravure coating of a photocurable epoxy resin onto a PET film and bonding to the graphene/copper foil, followed by curing of the epoxy resin. Figure 7c shows spray etching of the copper foil with a $CuCl_2$ solution, and Fig. 7d illustrates the final structure of the fabricated graphene/ epoxy/PET film. More details on the entire process flow can be found elsewhere.[135]

An alternative method of removing the grown graphene from Cu is shown in the three-step roll-to-roll transfer process in Fig. 8. A thermal release tape is first attached to the graphene film grown on the Cu foil, and then the Cu foil is etched in a reactive bath. The graphene film is then rinsed with deionized water to remove residual etchant. Exposing the graphene film on the polymer support to mild heat leads to the transfer of graphene from polymer to the target substrate.[136,137] The electrical quality of produced graphene films was then improved by multiple stacking and wet chemical doping using $AuCl_3$–CH_3NO_2 (more details can be found elsewhere[136]). Doped graphene films with four layers in average with a resistance as low as ~43 Ohm/sq and a transmittance of ~89 % were prepared by repeating these steps on the same substrate.

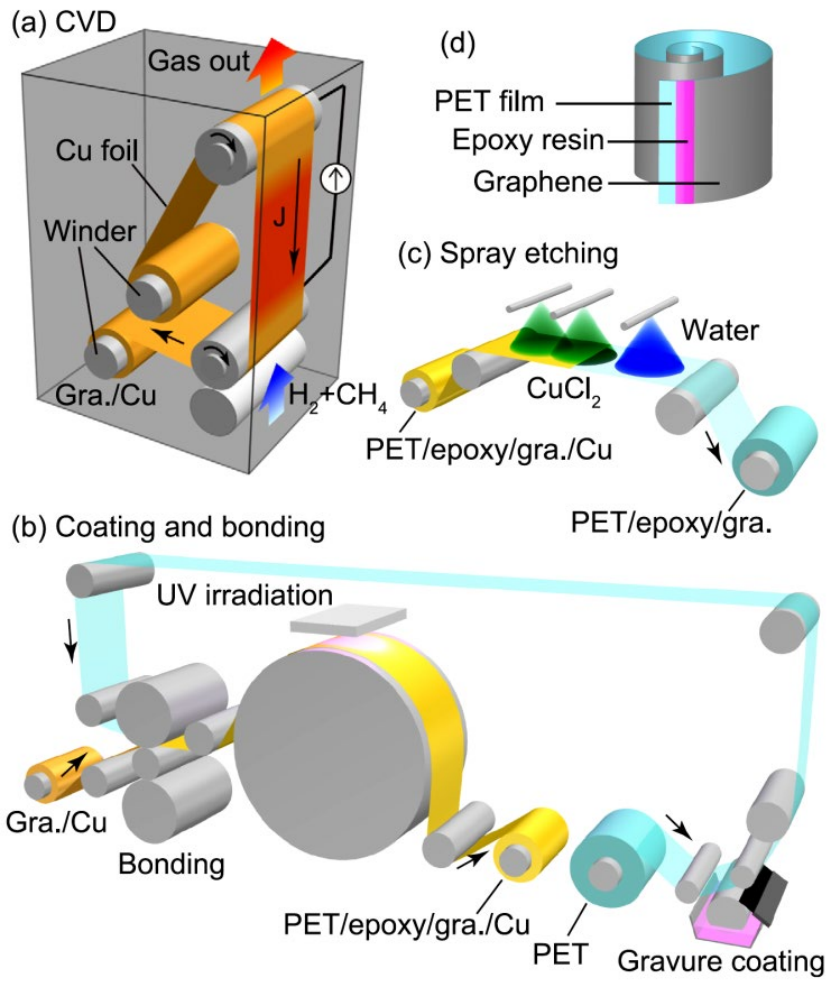

Fig. 7 (a) Continuous roll-to-roll CVD system using selective Joule heating to heat a copper foil suspended between two current-feeding electrode rollers to 1000 °C to grow graphene on copper. (b) Reverse gravure coating of a photocurable epoxy resin onto a PET film and bonding to the graphene/copper foil, followed by curing of the epoxy resin. (c) Spray etching of the copper foil with a $CuCl_2$ solution. (d) Structure of the fabricated graphene/epoxy/PET film. Reprinted with permission from T. Kobayashi et al. Appl. Phys. Lett. 102, 023112 (2013). Copyright 2013, American Institute of Physics.

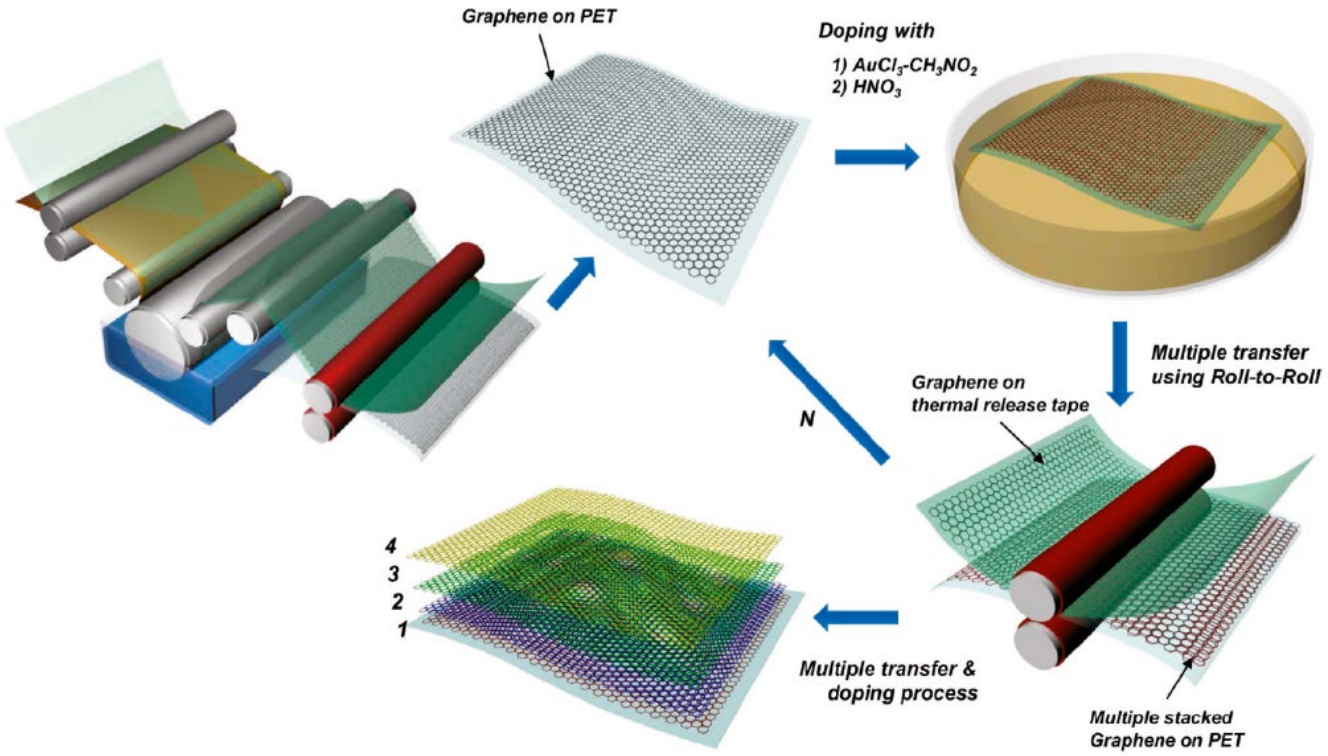

Fig. 8 A schematic of the fabrication procedures for preparing transparent flexible graphene films with layer-by-layer doping methods. The interlayer-doped graphene films are exposed to two wet chemical p-dopants, such as $AuCl_3$–CH_3NO_2 and HNO_3, after each layer is transferred, leading to the low sheet resistance as low as ~43 Ohm/sq with ~89% optical transmittance. Reprinted with permission from J. Kang et al., Nano Lett. 2011, 11, 5154. Copyright 2013, American Chemical Society.

Plasma-based roll-to-roll systems for the large-scale graphene production can be designed using similar concepts and designs, but incorporating the relevant plasma sources. One of the existing systems of this kind, based upon microwave PECVD, is sketched in Fig. 9.[138] The plasma was generated using eight coaxial linear air-cooled antennas covered with quartz tubes. This setup comprised two microwave generators with the power output of 20 kW. Methane, hydrogen and argon supplied from the top of chamber were used as source gases. The system comprises winder and un-winder sections as shown in Fig. 9.

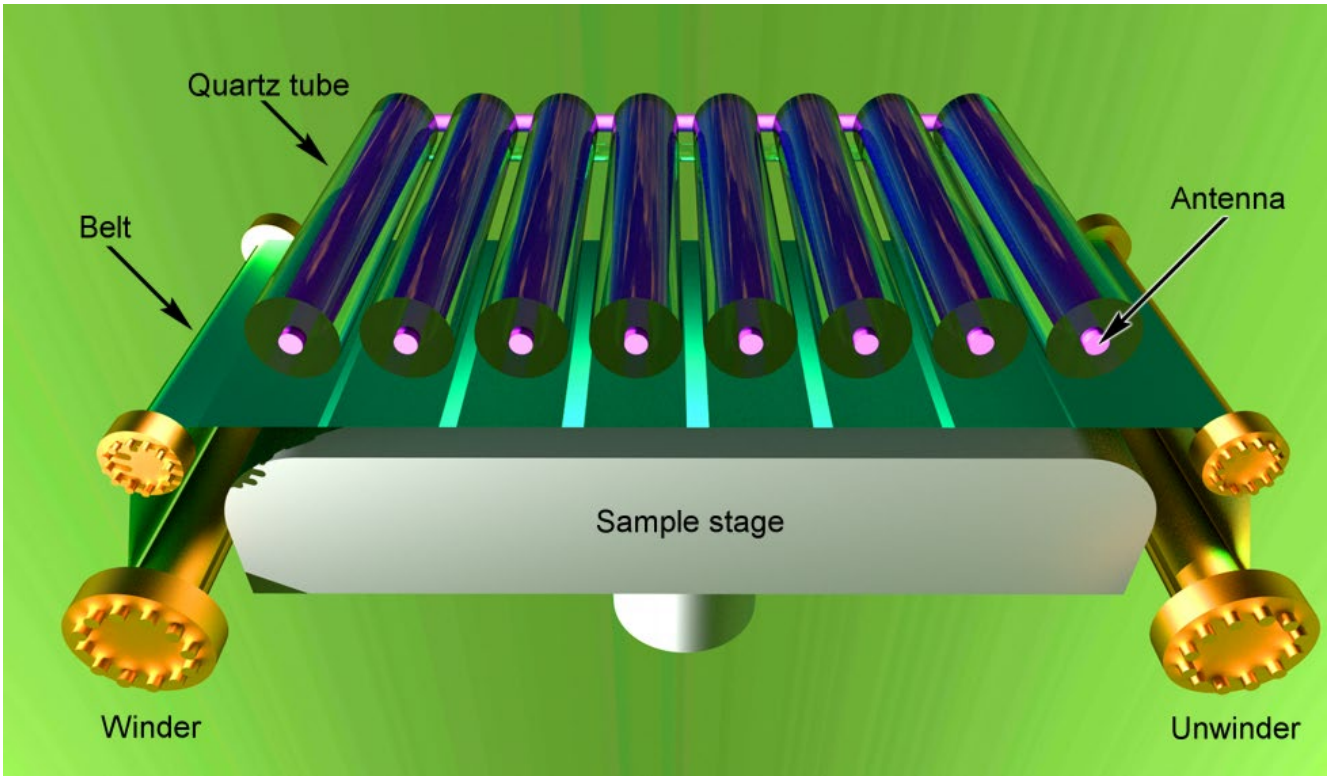

Fig. 9 Schematic of the roll-to-roll plasma-enhanced CVD set-up for the continuous graphene deposition. The lengths of antennas and quarts tubes do not have strong physical limits, and thus the width of the belt carrying the graphene films may potentially reach several meters. The length of the active plasma zone also does not have physical limits but may be limited by the energy cost and production plant geometrical sizes. The length of the roll is limited by the maximum winder/revinder loads, commercial availability of sufficiently long rolls, and process cost considerations. The size of the vacuum chamber is a major limiting factor for the scale-up. A major challenge is therefore to implement a similar process without relying on vacuum and expensive vacuum-grade chambers and airlocks.

The Cu foil speed during the process is maintained within 500 mm/s. The sample holder where deposition takes place is about 0.5 m in length. The deposited graphene thickness can be controlled by the foil speed. The temperature is maintained in the range of 100 to 400 °C by changing the distance between the quartz tubes and the substrate holder. Continuous films can be deposited in this system at substrate transfer speed of 5 $mm \times s^{-1}$ and temperature of about 400°C and the total microwave power

coupled to the system is ~16 kW. Importantly, the rolled 33 μm-thick Cu foil is commercially produced and thus represents an inexpensive substrate compared to other metal materials. More details can be found elsewhere.[138]

Such systems can be used for the fabrication of graphene structures on the whole device, e.g., flexible roll-out thin-film solar cell panels[139] of several square meter area suitable for the space[140] and field applications.[141] The size limitations of the plasma-based R2R production facilities are imposed by the lengths of the plasma discharges, sizes of the vacuum chamber(s), and other (e.g., process cost) considerations. See caption to Fig. 9 for more details.

The plasma-based roll-to-roll systems for large-scale graphene production could suffer from some problems intrinsic to the plasma-based process environment. Some of the most important issues to be solved are:

1) Possible non-uniform distribution of the plasma density and other important parameters over the large treatment area,[142] which eventually will deteriorate the quality and quantity of graphene synthesized on the plasma-exposed surfaces. Indeed, the conditions of nucleation and growth rates of nanostructures are very sensitive to the plasma parameters[143,144] and could be affected by, e.g., slight changes in the energy of ions extracted from the plasma bulk through the plasma-surface sheath.[145,146] This problem could be solved, firstly, by the use of a large number of small plasma sources (antennas); and secondly, by the use of sophisticated magnetic systems to control and re-distribute the plasma fluxes over the large surface areas.[147,148] However, these solutions will inevitably lead to the higher capital costs of the production equipment.

2) Possible overheating of the substrate (heat sensitive polymer films are often used as substrates for, e.g., transparent solar cell arrays). Intense ion bombardment from dense plasmas facilitates nucleation and fast growth of the graphene film on the metal foil, but simultaneously could easily damage and even melt the foil. Consequently, additional cooling arrangements or remote plasma configurations (where the substrate exposure to the plasma ions is reduced) may be necessary to minimize the damage to the polymer film. An advantage of the plasma-based process is the possibility to control the film temperature by the plasma parameters.

Let us now discuss the possible principle of operation and possible conceptual design of the apparatus for the continuous production of the unsupported (not bound to the substrate surface) graphene flakes (and carbon nanotubes as by-product) in arc discharge plasmas. Such a product is usually thought to be a base for the electrically conductive inks suitable for the large-scale production of printed electronic circuit boards, energy storage, flexible photovoltaic and other devices.[149] A potential solution should involve the following production stages (and hence, the appropriate set of hardware units) integrated in a single process (Fig. 10):

1) The gas, catalyst powder and power supply unit. This module should provide the gas and the catalyst (for example, Y-Ni powder), as well as electric power (low-voltage DC, not exceeding 100 V) supply into the chamber. The catalyst in the experimental setup may be packed directly in the consumable electrode,[150] but catalyst powder dispersion into a gas flow should be a better solution for the large-scale continuously operating installation. As it was mentioned above, the catalyst may be avoided by using the proper substrate temperature.[118]

2) The process unit consisting of the reaction (growth) chamber, cathode, anode, product collection surface and the optional magnetic system responsible for the process intensification and graphene-nanotube separation. The arc discharge between the anode and cathode is sustained in the volume of the reaction chamber, graphene flakes are nucleated on the plasma-treated (heated up and activated) catalyst particles, grow in the plasma (with the very high growth rate[113]) and eventually deposit on the collection surfaces inside the chamber. When the magnetic system is used, graphene flakes are deposited separately of the carbon nanotubes; otherwise, they can be separated later by, e.g. ultrasonication.[151,152] The collection surfaces may be installed onto a looped belt used to remove the ready deposit from the chamber as sketched in Fig. 10;

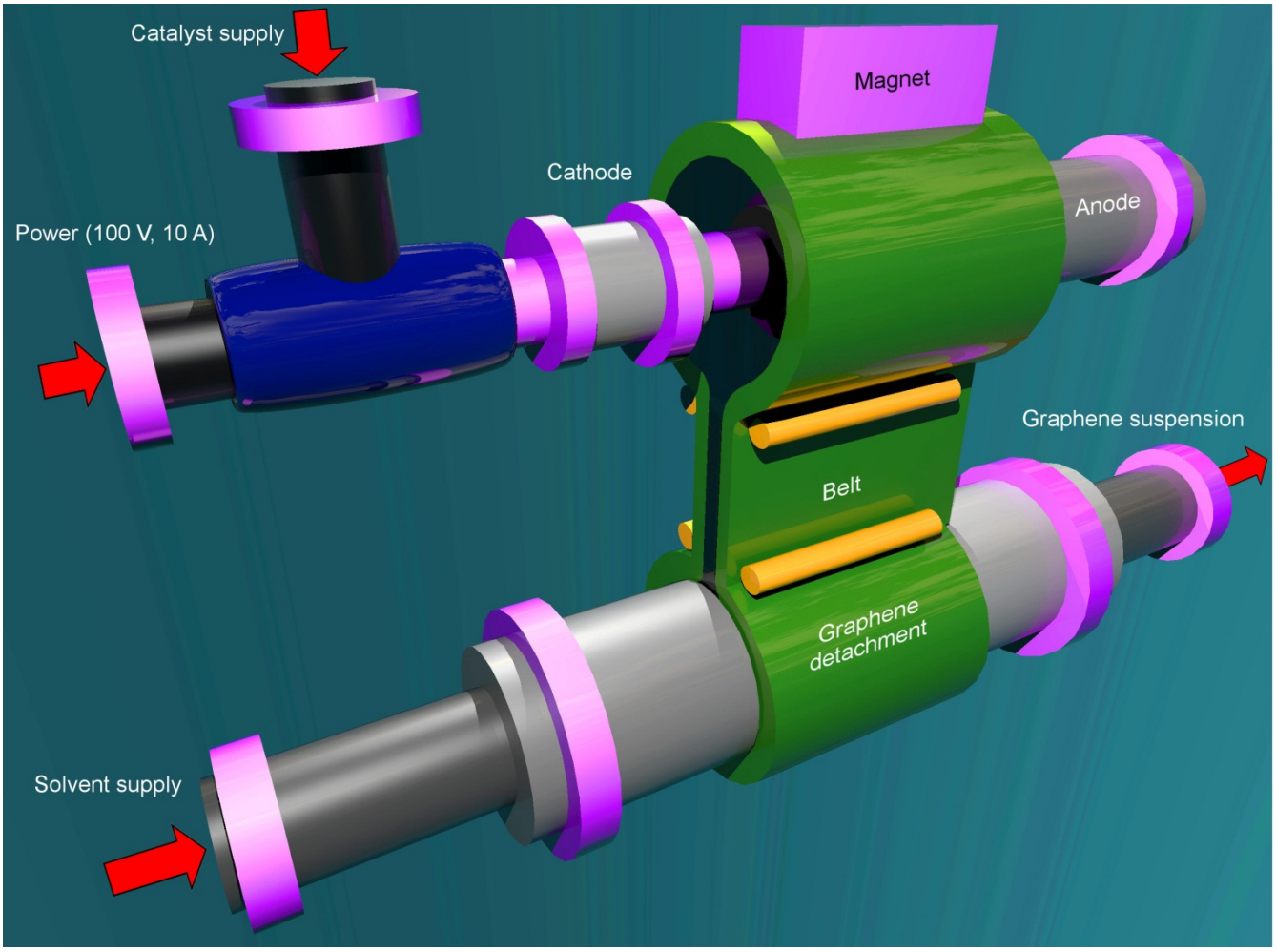

Fig. 10 Concept of the large-scale graphene production system based on arc discharge. The whole apparatus can be sub-divided to several sub-units: catalyst, gas and power supply unit; process unit (chamber, cathode, anode, magnet); product transportation unit (belt with the necessary guide rolls and actuators), and graphene suspension preparation unit (chamber with solvent washing out the graphene product from the belt, and container for the suspension).

3) The product transportation unit consisting of an infinite (closed loop) belt with the necessary guide rolls and actuators. The graphene flakes produced in the reaction chamber are deposited on the inside surface of the moving belt and then are removed from the chamber. Importantly, the arc discharge graphene synthesis can be conducted at the high enough (up to atmospheric) pressures (but still not in the oxygen-containing atmosphere), and hence, no complex airlock chambers are required to feed the belt out of the chamber;
4) The belt with the graphene deposit should be moved into the graphene suspension preparation unit consisting of a chamber where the graphene product is washed from the belt surface using solvent, and accumulated in the container for the graphene suspension. The suspension could be used, e.g., for the printable ink preparation[153] or further functionalization.[154] Additional process steps may be required to provide the suspension density required for the conducting ink to be printed with the required mass loading or other factors important for the expected device performance in applications.

We should stress that the s system shown in Figure 10 is a concept rather than an existing design. Nevertheless, the described concept is mostly based on the existing and already tested equipment and units. The base sub-systems such as arc-based graphene production unit, sonification system and some others are actually existing and working laboratory equipment which can be in principle combined into a single system using the components which do not require thorough research and development efforts. We agree that improvements in operational design may be required to produce a viable system, however the component composition and logic of their interaction follows from the physics of graphene nucleation and growth and hence, it should be put into the base of any similar device.

Plasmas could be used to further improve the output. Graphene patterning based on electron-beam or ultraviolet lithography and lift-off technique is one of the many examples of the potentially scalable methods featuring high levels of pattern resolution and simplicity.[155,156] Plasma activation and cleaning may be potentially considered as a way to enhance the product quality in the method. Finally, plasmas can be used to functionalise the graphene with, for example, hydroxyl groups to enhance the solubility of graphene in water or common polymer matrices.

5 Safety considerations

Safety of the graphene production technologies is an important issue due to many potentially hazardous chemicals and substances involved in the process. Among others, the plasma-based technologies could be considered as substantially environment-benign methods. Indeed, the most part of plasma-based technological processes is conducted in closed reactors, in vacuum or controlled environment, and hence, many potential hazards are not present (Fig. 11).[157] Specifically, graphenes are not fabricated in open air due to too high oxygen content which can significantly deteriorate the quality of graphene product. Instead, specific gas mixtures involving inert and carbon-containing gases and gas mixtures are used, and the enclosed process reactors prevent the leak of the process products which are exhausted using the vacuum system. The human respiratory tract is isolated from the contact with volatile hazardous substances, as well as liquids and other chemicals during the whole process. The produced graphene products also remain in the chamber without a contact with humans.

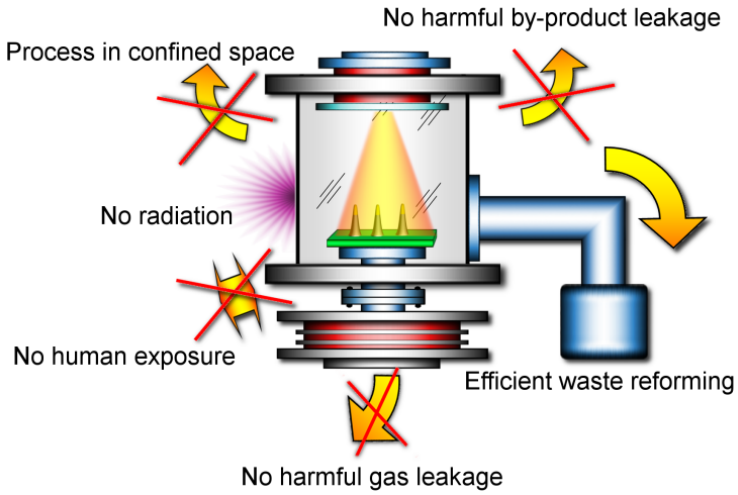

Fig. 11 Plasma-based technological processes are usually conducted in confined reactor chambers. The breathing zone of the researcher remains isolated from the harmful volatile compounds, and no toxic gas or liquid chemicals can be exposed to humans. No radiation is present outside the chamber, no harmful gas leakage and harmful by-products. Reprinted with permission from Han et al., "Plasma nanofabrication and nanomaterials safety", J. Phys. D: Appl. Phys. 44, 174019 (2011).

Concluding remarks

In this paper, we have briefly discussed the possibilities, trends and challenges in applications of low-temperature plasmas in scalable production of graphenes and related materials. We have considered the techniques for the production of three typical types of graphenes, namely surface-supported oriented flakes (commonly termed nanowalls, vertical graphenes, or vertically-aligned graphenes), free-standing (unsupported) graphene flakes and substrate-supported films. While examining the plasma-based graphene production methods, we have mainly focused on the inductively-coupled plasma and arc discharges-based techniques. Low-temperature plasmas have a significant potential to enhance many existing graphene fabrication techniques. Such plasmas show many unique properties such as high densities of reactive species resulting in high film/flake growth rates, as well as higher (yet controllable) ion and electron energies favourable for the effective cleaning and activation of the growth surfaces.

Many questions and issues remain open and stimulate future research and innovative solutions. By combining the advantages offered by conventional techniques with the versatility of plasma deposition, new ways for scaling the graphene production can be envisaged. Nevertheless, a substantial effort is required to eventually translate the exciting properties of graphenes into technological and commercial reality.[158,159,160]

Acknowledgements

This work was partially supported by CSIRO's OCE Science Leadership Program and the Australian Research Council.

References

1 K. S. Novoselov, D. Jiang, F. Schedin, T. J. Booth, V. V. Khotkevich, S. V. Morozov and A. K. Geim, *Proc. Natl. Acad. Sci. USA,* 2005, **102**, 10451.

2 Intellectual Property Office 2015, "Graphene. The worldwide patent landscape in 2015" (www.ipo.gov.uk/informatics)

3 A. Zurutuza and C. Marinelli, Challenges and opportunities in graphene commercialization, *Nature Nanotech.,* 2014, **9**, 730.

4 M. Keidar, Y. Raitses, A. Knapp and A. Waas, *Carbon,* 2006, **44**, 1022.

5 J. M. Hawkins, A. Meyer, T. A. Lewis, S. Loren and F. J. Hollander, *Science,* 1991, **12**, 312.

6 J. Baringhaus, J. Aprojanz, J. Wiegand, D. Laube, M. Halbauer, J. Hubner, M. Oestreich and C. Tegenkamp, *Appl. Phys. Lett.,* 2015, **106**, 043109.

7 A. Taroni, *Nature Mater.,* 2013, **12**, 778.

8 N. Domun, Hadavinia, T. Zhang, T. Sainsbury, G. H. Liaghat and S. Vahid, *Nanoscale,,* 2015, **7**, 10294.

9 K. Kostarelos and K. S. Novoselov, *Nature Nanotechnol.,* 2014, **9**, 744.

10 Y. Shao, J. Wang, H. Wu, J. Liu, I. A. Aksay, Y. Lin, *Electroanalysis,* 2010, **22**, 1027.

11 J.-H. Ahn and B. H. Hong, *Nature Nanotechnol.,* 2014, **9**, 737.

12 V.-D. Dao, L. L. Larina, K.-D. Jung, J.-K. Lee and H.-S. Choi, *Nanoscale,* 2014, **6**, 477.

13 F. Torrisi and J. N. Coleman, *Nature Nanotechnol.,* 2014, **9**, 738.

14 R. Raccichini, A. Varzi, S. Passerini and B. Scrosati, *Nature Mater.,* 2015, **14**, 271.

15 M. Pumera, *Chem. Rec.,* 2009, **9**, 211.

16 S. Böhm, *Nature Nanotechnol.,* 2014, **9**, 741.

17 E. J. Siochi, *Nature Nanotechnol.,* 2014, **9**, 745.

18 S. Lee, J.-Y. Hong and J. Jang, *ACS Nano*, 2013, **7,** 5784.

19 L. Vicarelli, M. S. Vitiello, D. Coquillat, A. Lombardo, A. C. Ferrari, W. Knap, M. Polini, V. Pellegrini and A. Tredicucci, *Nature Mater.*, 2012, **11**, 865.

20 U. G. K. Wegst, H. Bai, E. Saiz, A. P. Tomsia and R. O. Ritchie, *Nature Mater.*, 2015, **14**, 23.

21 D. Seo, S. Yick, S. Pineda, D. Su, G. Wang, Z. Han, K. Ostrikov, *ACS Sustainable Chem. Eng.,* 2015, **3**, 544.

22 D. H. Seo, Z. J. Han, S. Kumar, K. Ostrikov, *Adv. Energy Mater.,* 2013, **3**, 1316.

23 V. Singh, D. Joung, L. Zhai, S. Das, S. I. Khondaker and S. Seal, *Progress in Mater. Sci.,* 2011, **56**, 1178.

24 J. Wang, M. Y. Zhu, R. A. Outlaw, X. Zhao, D. M. Manos and B. C. Holoway, *Carbon,* 2004, **42**, 2867.

25 D. R. Cooper, B. D'Anjou, N. Ghattamaneni, B. Harack, M. Hilke, A. Horth, N. Majlis, M. Massicotte, L. Vandsburger, E. Whiteway and V. Yu, *ISRN Condens. Matter Phys.,* 2012, **2012**, 501686.

26 K. Ostrikov, E.C. Neyts and M. Meyyappan, *Adv. Phys.,* 2013, **62**, 113.

27 I. Levchenko, M. Keidar, S. Xu, H. Kersten and K. Ostrikov, *J. Vac. Sci. Technol. B,* 2013, **31**, 050801.

28 D. V. Szabo and S. Schlabach, *Inorganics,* 2014, **2**, 468.

29 D. Pappas, *J. Vac. Sci. Technol.A* 2011, **29**, 020801.

30 E. R. Fisher, *Plasma Proc. Polym.,* 2004, **1**, 13.

31M. A Lieberman and A. J. Lichtenberg, *Principles of Plasma Discharges and Materials processing*, John Wiley & Sons, 2005, Hoboken, New Jersey.

32 H. B. Profijt, S. E. Potts, M. C. Sanden and W. M. M. Kessels, *J. Vac. Sci. Technol. A.* 2011, **29**, 050801.

33 A. Anders, *Cathodic Arcs: From Fractal Spots to Energetic Condensation*, Springer, New York, 2008.

34 F. F. Chen, *Phys. Plasmas,* 1995, **2**, 2164.

35 M. J Kushner, *J. Phys. D: Appl. Phys.,* 2009, **42** 194013.

36 S. Samukawa, M. Hori, S. Rauf, K. Tachibana, P. Bruggeman, G. Kroesen, J. Ch. Whitehead, A. B. Murphy, A. F. Gutsol, S. Starikovskaia, U. Kortshagen, J.-P. Boeuf, T. J. Sommerer, M. J. Kushner, U. Czarnetzki and N. Mason, *J. Phys. D: Appl. Phys.*, 2012, **45**, 253001.

37 A. Bendavid and P.J. Martin, *J. Austral. Ceram. Soc.*, 2014, **50**, 86.

38 J. M. Lafferty, *Vacuum Arcs – Theory and Applications,* New York: Wiley, 1980.

39 J. Kim and J. S. Suh, *ACS Nano,* 2014, **8**, 4190.

40 S. Unarunotai, Y. Murata, C. E. Chialvo, H.-s. Kim, S. MacLaren, N. Mason, I. Petrov and J. A. Rogers, *Appl. Phys. Lett.,* 2009, **95**, 202101.

41 C. Botas, A. M. Pérez-Mas, P. Álvarez, R. Santamaría, M. Granda, C. Blanco and R. Menéndez, *Carbon,* 2013, **63**, 576.

42 T. Fan, W. Zeng, W. Tang, C. Yuan, S. Tong, K. Cai, Y. Liu, W. Huang, Y Min and A. J. Epstein, *Nanoscale Res. Lett.,* 2015, **10**, 55.

43 I. Vlassiouk, S. Smirnov, S. P. Surwade, M. Regmi, N. Srivastava, R. Feenstra, G. Eres, C. Parish, N. Lavrik, P. Datskos, S. Dai and P. Fulvio, *J. Phys. Chem. C,* 2013, **117**, 18919.

44 A. Reina. X. Jia, J. Ho, D. Nezich, H. Son and V. Bulovic, *Nano Lett.,* 2009, **9**, 30.

45 X. Li, C. W. Magnuson, A. Venugopal, J. An, J. W. Suk, B. Han, M. Borysiak, W. Cai, A, Velamakanni, Y. Zhu, L. Fu, E. M. Vogel, E. Voelkl, L. Colombo and R. S. Ruoff, *Nano Lett.,* 2010, **10**, 4328.

46 X. Li, C. W. Magnuson, A. Venugopal, R. M. Tromp, J. B. Hannon, E. M. Vogel, L. Colombo and R. S. Ruoff, *J. Am. Chem. Soc.,* 2011, **133**, 2816.

47 S. Kumar, I. Levchenko, Q. J. Cheng, J. Shieh and K. Ostrikov, *Appl. Phys. Lett.,* 2012, **100**, 053115.

48 Y. S. Kim, J. H. Lee, Y. D. Kim, S.-K. Jerng, K. Joo, E. Kim, J. Jung, E. Yoon, Y. D. Park, S. Seo and S.-H. Chun, *Nanoscale,* 2013, **5**, 1221.

49 S. Kumar, T. Laan, A. E. Rider, L. Randeniya and K. Ostrikov, *Adv. Funct. Mater.,* 2014, **24**, 6114.

50 D. A. Boyd, W.-H. Lin, C.-C. Hsu, M. L. Teague, C.-C. Chen, Y.-Y. Lo, W.-Y. Chan, W.-B. Su, T.-C. Cheng, C.-S. Chang, C.-I. Wu and N.-C. Yeh, *Nature Comm.*, 2012, **6**, 6620.

51 S.Kumar, K. Ostrikov, *Nanoscale,* 2011, **3**, 4296.

52 J. Fang, I. Levchenko, S. Kumar, D. Seo and K. Ostrikov, *Sci. Technol. Adv. Mater.,* 2014, **15**, 055009.

53 Y. Wu, B. Wang, Y. Ma, Y. Huang, N. Li, F. Zhang and Y. Chen, *Nano Res.,* 2010, **3**, 661.

54 K. S. Subrahmanyam, L. S. Panchakarla, A. Govindaraj and C. N. R. Rao, *J. Phys. Chem. C.,* 2009, **113**, 4257.

55 C. Wu, G. Dong, L. Guan, *Physica E.,* 2010, **42**, 1267.

56 Y. Li, Q. Chen, K. Xu, T. Kaneko and R. Hatakeyama, *Chem. Eng. J.,* 2013, **215**, 45.

57 L. Huang, B. Wu, J. Chen, Y. Xue, D. Geng, Y. Guo, G. Yu and Y. Liu, *Small,* 2013, **9**, 1330.

58 I. Levchenko, O. Volotskova, A. Shashurin, Y. Raitses, K. Ostrikov and M. Keidar, *Carbon,* 2010, **48**, 4570.

59 A. K. Geim and K. S. Novoselov, *Nat. Mater.,* 2007, **6**, 183.

60 A. Reina, X. Jia, J. Ho, D. Nezich, H. Son, V. Bulovic, M. Dresselhaus and J. Kong, *Nano Lett.* 2009, **9**, 30.

61 L. G. De Arco, Y. Zhang, A. Kumar and C. Zhou, *IEEE Trans. Nanotechnol.,* 2009, **8**, 135.

62 T. Moldt, A. Eckmann, P. Klar, S. V. Morozov, A. A. Zhukov, K. S. Novoselov and C. Casiraghi, *ACS Nano,* 2011, **5**, 7700.

63 A. Balan, R. Kumar, M. Boukhicha, O. Beyssac, J.-C. Bouillard, D. Taverna, W. Sacks, M. Marangolo, E. Lacaze, R. Gohler, W. Escoffier, J.-M. Poumirol and A. Shukla, *J. Phys. D: Appl. Phys.,* 2010, **43**, 374013.

64 T. N. Lin, K. H. Chih, C. T. Yuan, J. L. Shen, C. A. J. Lin and W. R. Liu, *Nanoscale,* 2015, **7**, 2708.

65 A. Dahal and M. Batzill, *Nanoscale,* 2014, **6**, 2548.

66 L. Baraton, Z. B. He, C. S. Lee, C. S. Cojocaru, M. Châtelet, J.-L. Maurice, Y. H. Lee and D. Pribat, *Europhys. Lett.,* 2011, **96**, 46003.

67 H. Mao, F. Hu, Q.-L. Ye, Y. Xu, X. Yang and B. Lu, *Nanoscale,* 2014, **6**, 8149.

68 Y. Hernandez, V. Nicolosi, M. Lotya, F. M. Blighe, Z. Sun and S. De, *Nature Nanotechnol.,* 2008, **3**, 563.

69 L. Zhu, X. Zhao, Y. Li, X. Yu, C. Li and Q. Zhang, *Mat. Chem. Phys.,* 2013, **137**, 984.

70 F. Bonaccorso, A. Lombardo, T. Hasan, Z. Sun, L. Colombo, A. C. Ferrari, *Mat. Today,* 2012, **15**, 564.

71 H. J. Song, M. Son, C. Park, H. Lim, M. P. Levendorf, A. W. Tsen, J. Park and H. C. Choi, *Nanoscale,* 2012, **4**, 3050.

72 H. Tian, Y. Shu, Y.-L. Cui, W.-T. Mi, Y. Yang, D. Xie and T.-L. Ren, *Nanoscale,* 2014, **6**, 699.

73 Y. L. Zhong, Z. Tian, G. P. Simon and D. Li, *Mat. Today,* 2015, **18**, 73.

74 K. R. Paton, E. Varrla, C. Backes, R. J. Smith, U. Khan, A. O'Neill, C. Boland, et al. *Nature Mater.,* 2014, **13**, 624.

75 D. Wei, Y. Liu, H. Zhang, L. Huang, B. Wu, J. Chen and G. Yu, *J. Am. Chem. Soc.,* 2009, **131**, 11147.

76 Z. L. Tsakadze, I. Levchenko, K. Ostrikov and S. Xu, *Carbon,* 2007, **45,** 2022.

77 R. M. Sankaran and W.-H. Chiang, *Nat. Mater.,* 2009, **8**, 882.

78 I. Levchenko, S. Y. Huang, K, Ostrikov and S. Xu, *Nanotechnol.* 2010*,* **21**, 025605.

79 K. Davami, M. Shaygan, N. Kheirabi, J. Zhao, D. A. Kovalenko, M. H. Rummeli, J. Opitz, G. Cuniberti, J.-S. Lee and M. Meyyappan, *Carbon,* 2014, **72**, 372.

80 I. Levchenko and K. Ostrikov, *Nanotechnol*. 2008, **19**, 33570.

81 U. Khalilov, A. Bogaerts, E. C. Neyts, *Nanoscale,* 2014, **6**, 9206.

82 I. Levchenko and K. Ostrikov, *J. Phys. D: Appl. Phys.,* 2007, **40**, 2308.

83 E. A. Anumol, B. Viswanath, P. G. Ganesan, Yunfeng Shi, Ganpati Ramanath and N. Ravishankar, *Nanoscale,* 2010, **2**, 1423.

84 I. Levchenko, K Ostrikov and A B Murphy, *J. Phys. D: Appl. Phys.,* 2008, **41**, 092001.

85 P. G. Mani-Gonzalez, M. O. Vazquez-Lepe and A. Herrera-Gomez, *J. Vac. Sci. Technol. A* 2015, **33**, 010602.

86 Z. Ren, N. Meng, K. Shehzad, Y. Xu, S. Qu, B. Yu and J. K. Luo, *Nanotechnology,* 2015, **26,** 065706.

87 Z. Bo, Y. Yang, J. Chen, K. Yu, J. Yan and K. Cen, *Nanoscale,* 2013, **5**, 5180.

88 I. Levchenko, K. Ostrikov, D. Mariotti and A. B. Murphy, *J. Appl. Phys.,* 2008, **104**, 073308.

89 H.-S. Tsai, C.-C. Lai, H. Medina, S.-M. Lin, Y.-C. Shih, Y.-Z. Chen, J.-H. Liang and Y.-L. Chueh, *Nanoscale,* 2014, **6**, 13861.

90 Z. Bo, Y. Yang, J. Chen, K. Yu, J. Yan and K. Cen, *Nanoscale,* 2013, **5**, 5180.

91 D. W. Yue, C. H. Ra, X. C. Liu, D. Y. Lee and W. J. Yoo, *Nanoscale,* 2015, **7**, 825.

92 O. Volotskova, I. Levchenko, A. Shashurin, Y. Raitses, K. Ostrikov and M. Keidar, *Nanoscale,* 2010, **2**, 2281.

93 C. Wang, Y. Zhou, L. He, T.-W. Ng, G. Hong, Q.-H. Wu, F. Gao, C.-S. Lee and W. Zhang, *Nanoscale,* 2013, **5**, 600.

94 D. Z. Pai, K. Ostrikov, S. Kumar, D. A. Lacoste, I. Levchenko and C. O. Laux, *Sci. Rep.,* 2013, **3**, 1221.

95 D. Mariotti and R. M. Sankaran, *J. Phys. D-Appl. Phys.,* 2010, **43**, 323001.

96 T. Nozaki, K Sasaki, T. Ogino, D. Asahi and K. Okazaki, *Nanotechnology,* 2007, **18**, 235603.

97 D. Mariotti, H. Lindstrom, A. C. Bose and K Ostrikov, *Nanotechnology,* 2008, **19**, 495302.

98 Y. Shimizu et al*., Jpn. J. Appl. Phys. Part 1 - Regul. Pap. Brief Commun. Rev. Pap.,* 2006, **45**, 8228.

99 J. Chen, G. Lu, L. Zhu and R. C. Flagan, *J. Nanopart. Res.,* 2007, **9**, 203.

100 N. S. Tabrizi, M. Ullmann, V. A. Vons, U. Lafont and A. Schmidt-Ott, *J. Nanopart. Res.,* 2009, **11**, 315.

101 D. Z. Pai, *J. Phys. D.: Appl. Phys.,* 2011, **44**, 174024.

102 M. Segal, *Nature Nanotech.,* 2009, **4**, 612.

103 M. Xu, D. Fujita, K. Sagisaka, E. Watanabe and N. Hanagata, *ACS Nano,* 2011, **5**, 1522.

104 Y. Hernandez, V. Nicolosi, M. Lotya, F. M. Blighe, Z. Sun, S. De, I. T. Mcgovern, B. Holland, M. Byrne, Y. K. Gunko et. al., *Nature Nanotechnol.,* 2008, **3**, 563.

105 K. Kobayashi, M. Tanimura, H. Nakai, A. Yoshimura, H. Yoshimura, K. Kojima and M. Tachibana, *J. Appl. Phys.,* 2007, **101**, 094306.

106 T. H. Chuang, B. O. Boskovic and J. Robertson, *Diamond Relat. Mater.,* 2006, **15**, 1103.

107 A. Chuang, J. Robertson, B. Boskovic and K. Koziol, *Appl. Phys. Lett.,* 2007, **90**, 123107.

108 A. Dato, V. Radmilovic, Z. H. Lee, J. Phillips and M. Frenklach, *Nano Lett.,* 2008, **8**, 2012.

109 I. Levchenko, O. Volotskova, A. Shashurin, Y. Raitses, K. Ostrikov and M. Keidar, *Carbon,* 2010, **48**, 4570.

110 S. Karmakar, N. V. Kulkarni, A. B. Nawale, N. P. Lsalla, R. Mishra and V. G. Sathe, *J. Phys. D. Appl. Phys.,* 2009, **42**, 115201.

111 M. Keidar and I. Belis, *J. Appl. Phys.,* 2009, **106,** 103304.

112 A. B. Murphy, *J. Phys. D: Appl. Phys.,* 2013, **46,** 224004.

113 K. Anazawa, K. Shimotani, C. Manabe, H. Watanabe, M. Shimizu, *Appl. Phys. Lett.,* 2002, **81**, 739.

114 M. Keidar, I. Levchenko, T. Arbel, M. Alexander, A. M. Waas and K. Ostrikov, *Appl. Phys. Lett.,* 2008, **92**, 043129.

115 A. Shashurin and M. Keidar, *J. Phys. D: Appl. Phys.*, 2015, **48**, 314007.

116 M. Keidar, I. Levchenko, T. Arbel, M. Alexander, A. M. Waas and K. Ostrikov, *J. Appl. Phys.,*2008, **103**, 094318.

117 M. Keidar, A. M. Waas, Y. Raitses and E. Waldorff, *J. Nanosci. Nanotechnol.* 2006, **6**, 1309.

118 O. Volotskova, A. Shashurin, M. Keidar, Y. Raitses, V. Demidov and S. Adams, *Nanotechnol*. 2010, **21**, 095705.

119 X. Fang, A. Shashurin and M. Keidar, *J. Appl. Phys.*, 2015, **118**, 103304.

120 E. B. Secor, P. L. Prabhumirashi, K. Puntambekar, M. L. Geier and M. C. Hersam, *Phys. Chem. Lett.,* 2013, **4**, 1347.

121 M. J. Behr, E. A. Gaulding, K. A. Mkhoyan and E. S. Aydil, *J. Vac. Sci. Technol. B* 2010, **28**, 1187.

122 I. Levchenko, K. Ostrikov, K. Diwan, K. Winkler and D. Mariotti, *Appl. Phys. Lett.,* 2008, **93**, 183102.

123 H. Kersten and G. M. W. Kroesen, *J. Vac. Sci. Technol. A* 1990, **8**, 38.

124 M. Hiramatsu, K. Shiji, H. Amano and M. Hori, *Appl. Phys. Lett.,* 2004, **84**, 4708.

125 D. H. Seo, S. Kumar and K. Ostrikov, *Carbon,* 2011, **49**, 4331.

126 Y. Wu, P. Qiao, T. Chong and Z. Shen, *Adv. Mater.,* 2002, **14**, 64.

127 I. Levchenko, M. Romanov and M. Keidar, *J. Appl. Phys.,* 2003, **94**, 1408.

128 B. Baitimbetova and B. Vermenichev, *Graphene,* 2015, **4**, 38.

129 I. Levchenko, M. Romanov, M. Keidar and I. I. Beilis, *Appl. Phys. Lett.,* 2004, **85**, 2202.

130 M. Hiramatsu, K. Shiji, H. Amano and M. Hori, *Appl. Phys. Lett.,* 2004, **84**, 4708.

131 C. Zhang, J. Hu, X. Wang, X. Zhang, H. Toyoda, M. Nagatsu and Y. Meng, *Carbon,* 2012, **50**, 3731.

132 Yang Y 2013 Mechanical properties of graphene with vacancy defects *Res. Mat. Sci.* **2** 50–57.

133 http://www.appliedmaterials.com

134 S.-S. Pei and W. Wu, *AAPPS Bulletin,* 2013, **23**, 4.

135 T. Kobayashi, M. Bando, N. Kimura, K. Shimizu, K. Kadono, N. Umezu, K. Miyahara, S. Hayazaki, S. Nagai, Y. Mizuguchi, Y. Murakami and D. Hobara, *Appl. Phys. Lett.,* 2013, **102**, 023112.

136 J. Kang, H. Kim, K. S. Kim, S.-K. Lee, S. Bae, J.-H. Ahn, Y.-J. Kim, J.-B. Choi and B. H. Hong, *Nano Lett.,* 2011, **11**, 5154.

137 J. A. Torres and R. B. Kaner, *Nature Mater.,* 2014, **13**, 328.

138 T. Yamada, M. Ishihara, J. Kim, M. Hasegawa and S. Iijima, *Carbon,* 2012, **50**, 2615.

139 G. Kalita, M. Matsushima, H. Uchida, K. Wakita and M. Umeno, *J. Mater. Chem.,* 2010, **20**, 9713.

140 S. H. Liu, E. J. Simburger, J. Matsumoto, A. Garcia, J. Ross and J. Nocerino, *Prog. Photovolt: Res. Appl.,* 2005, **13**, 149.

141 L. Dai, D. W. Chang, J.-B. Baek and W. Lu, *Small,* 2012, **8**, 1130.

142 I. Levchenko, M. Korobov, M. Romanov and M. Keidar, *J. Phys. D: Appl. Phys.,* 2004, **37**, 1690.

143 U. Khalilov, A. Bogaerts and E. C. Neyts, *Nanoscale,* 2014, **6**, 9206.

144 I. Levchenko, K. Ostrikov, D. Mariotti and V. Švrček, *Carbon,* 2009, **47**, 2379.

145 L. Seemann, A. Stemmer and N. Naujoks, *Nano Lett.,* 2007, **7**, 3007.

146 A. Felten, D. McManus, C. Rice, L. Nittler, J.-J. Pireaux and C. Casiraghi, *Appl. Phys. Lett.,* 2014, **105**, 183104.

147 O. Baranov, M. Romanov and K. Ostrikov, *Phys. Plasmas,* 2009, **16**, 053505.

148 G. Filipič, O. Baranov, M. Mozetič, K. Ostrikov and U. Cvelbar, *Phys. Plasmas,* 2014, **21**, 113506.

149 R. R. Søndergaard, M. Hösel and F. C. Krebs, *J. Polym. Sci. Part B: Polym. Phys.,* 2013, **51**, 16.

150 J. Li, A. Shashurin and M. Keidar, *IEEE Trans. Plasma Sci.,* 2011, **39**, 2366.

151 Y. Y. Huang and E. M. Terentjev, *Polymers* 2012, **4**, 275.

152 V. Chabot, B. Kim, B. Sloper, C. Tzoganakis and A. Yu, *Sci. Rep.,* 2013, **3**, 1378.

153 E. B. Secor, P. L. Prabhumirashi, K. Puntambekar, M. L. Geier and M. C. Hersam, *J. Phys. Chem. Lett.,* 2013, **4**, 1347.

154 X. Fang, J. Donahue, A. Shashurin , M. Keidar, *Graphene*, 2015, **4**, 1.

155 Y. Ye, L. Gan, L. Dai, Y. Dai, X. Guo, H. Meng, B. Yu, Z. Shi, et. al., *Nanoscale,* 2011, **3**, 1477.

156 M. Hofmann, Y.-P. Hsieh, A. L. Hsu and J.Kong, *Nanoscale,* 2014, **6**, 289.

157 Z. J. Han, I. Levchenko, S. Kumar, M. M. A.Yajadda, S. Yick, D. H. Seo, P. J. Martin, S. Peel, Z. Kuncic and K. Ostrikov, *J. Phys. D: Appl. Phys.,* 2011, **44**, 174019.

158 J. R. Miller, R. A. Outlaw and B. C. Holloway, *Science*, 2010, **329**, 1637.

159 J. Li, X. Cheng, J. Sun, C. Brand, A. Shashurin, M. Reeves and M. Keidar, *J. Appl. Phys.*, 2014, **115**, 164301.

160 Z. Bo,W. Zhu, W. Ma, Z. Wen, X. Shuai, J. Chen, J. Yan, Z. Wang, K. Cenand, X. Feng, *Adv. Mater.,* 2013, **25**, 5799.